Dual-Function WEC-Breakwater: Integrating Coastal Protection and Clean Energy Harvesting towards Net Zero

Hoang Quan Vu, Phan Thi Que Tran, and Assoc. Prof. Vo Ngoc Duong*
Faculty of Hydraulic Engineering
The University of Danang - University of Science and Technology
Danang, Vietnam
Vhquan0401@gmail.com, daly65541@gmail.com, vnduong@dut.udn.vn

Sylichantho Jolinar, Dang Cong Quoc Huy
Faculty of Architecture
The University of Danang - University of Science and Technology
Danang, Vietnam
josvp0218@gmail.com, Huydang18032003@gmail.com

Nguyen Thanh Ha, Dr. Doan Thi Ngoc Canh*
Faculty of E-commerce, Faculty of Statistics and Informatics
The University of Danang - University of Economics
Danang, Vietnam
bongcachua217@gmail.com, canhdtn@due.edu.vn

Le Thi Thu
Faculty of Electrical Engineering
The University of Danang - University of Science and Technology
Danang, Vietnam
Lethu25082003@gmail.com

Abstract - This study proposes a multifunctional coastal breakwater system that integrates wave attenuation, shoreline protection, and wave energy harvesting to generate renewable electricity for coastal applications. The system is developed for the coastal conditions of Quang Tri Province, Vietnam, where monsoon waves and storms impose large hydrodynamic loads on nearshore structures. Unlike conventional vertical breakwaters, which mainly reflect waves, the proposed system redistributes wave energy into reduced reflection, passive dissipation, and useful mechanical energy absorption. A three-dimensional numerical simulation based on the VOF (Volume of Fluid)) method is used to evaluate wave–structure interaction, pressure distribution, and hydrodynamic loads. The results show that the energy-absorbing breakwater can reduce the reflection coefficient by about 20–30% and wave loads by about 15–25% compared with a conventional breakwater. The absorbed energy is converted into electricity through a hydraulic PTO (Power Take-Off) system and a wave-to-wire architecture using a PMSG (Permanent Magnet Synchronous Generator) generator and an AC–DC–AC circuit. The system shows the potential to form sustainable coastal infrastructure that integrates wave attenuation, load reduction, and renewable power generation.

Keywords - Wave energy conversion; multifunctional coastal structures; wave–structure interaction; hydrodynamic loading; power take-off; coastal protection.

I. Introduction

Coastal areas are increasingly affected by climate change, sea-level rise, and extreme weather events, which intensify shoreline erosion and risks to nearshore infrastructure [1]. In Vietnam, the central coastal region is one of the most vulnerable areas because it is frequently affected by monsoon waves, storms, and longshore sediment transport. For Quang Tri Province, observational data from Con Co station show that the wave regime has a clear seasonal pattern; the annual mean wave height ranges from approximately 1.02 to 1.63 m, can reach 4–5 m under adverse conditions, and may increase to 6–9 m during strong storms [3]. This indicates an urgent need for coastal engineering solutions capable of reducing wave loads, limiting erosion, and adapting to harsh hydrodynamic conditions.

Conventional breakwaters currently operate mainly based on the mechanisms of wave reflection and wave energy dissipation. This mechanism can help protect the shoreline, but it also increases standing waves, hydrodynamic loads on the structure, and local scour at the breakwater toe [5]. Meanwhile, ocean wave energy is a renewable energy source with high energy density, relatively good predictability, and considerable exploitation potential in coastal areas with favorable wave conditions [6]. Therefore, instead of considering wave energy only as a load to be eliminated, a new approach is to develop multifunctional coastal structures that both attenuate waves for shoreline protection and absorb part of the wave energy for conversion into useful electricity.

In recent years, many studies have focused on optimizing coastal protection structures or developing wave energy conversion devices. However, these two research directions have largely been carried out independently. Coastal protection structures often have not fully considered the possibility of wave energy harvesting, while wave energy conversion devices have not been comprehensively integrated into nearshore infrastructure in terms of hydraulic, mechanical, electrical, operational, and long-term maintenance requirements in the marine environment [6], [8]. In particular, for the central coastal region of Vietnam, quantitative analyses of breakwaters integrated with wave energy within a multidisciplinary assessment framework remain limited.

On this basis, this study proposes a multifunctional coastal breakwater system that integrates wave attenuation, shoreline protection, and wave energy harvesting to generate renewable electricity for coastal applications. The study focuses on three main aspects: analyzing wave–structure interaction and the effectiveness of hydrodynamic load reduction; converting wave loads into input parameters for the hydraulic power take-off system; and proposing an electrical conversion architecture based on the wave-to-wire model. The main contribution of this study is to establish an integrated design framework combining hydraulics, mechanics, electrical engineering, and infrastructure architecture, thereby laying the foundation for the development of sustainable coastal structures capable of combining shoreline protection with renewable energy harvesting.

II. METHODOLOGY

A. Hydrodynamic Analysis and Wave–Structure Interaction.

1) Wave conditions and basis for selecting the study area..

The coastal area of Quang Tri Province is selected as a typical study area because it has a clear seasonal wave regime and is affected by the Northeast monsoon, the Southwest monsoon, and storm events from the East Sea. In this study, meteorological–oceanographic data are obtained from the CFSR (Climate Forecast System Reanalysis) reanalysis dataset of NCEP/NOAA (National Centers for Environmental Prediction/ National Oceanic and Atmospheric Administration) in combination with regional storm statistics, to determine wave characteristics under seasonal mean and extreme conditions [2], [3]. In winter, the Northeast monsoon generates a dominant wave field in the Northeast–East direction with a higher energy level; whereas in summer, the wave field decreases and changes direction under the influence of the Southwest monsoon. Observational data at Con Co show that the annual mean wave height ranges from approximately 1.02–1.63 m; under strong monsoon conditions, it can reach 4–5 m and up to 6–9 m during strong storms [3]. In addition, during the period 1996–2020, about 39 storms affecting Quang Tri were recorded, mainly concentrated from September to November, with common wind intensity of levels 9–12 [3]. These characteristics create a harsh hydrodynamic environment, suitable for evaluating the effectiveness of the breakwater system integrated with wave energy harvesting.

2) Energy balance basis and wave absorption mechanism.

When waves interact with a coastal structure, the incident wave energy is distributed into reflected, dissipated, and transmitted components through the structure. The dimensionless energy balance can be expressed as follows [4], [5]:

$$1 = K_r^2 + K_d^2 + K_t^2 \quad (1)$$

where K_r is the reflection coefficient, K_t is the wave transmission coefficient, and K_d^2 is the portion of energy dissipated due to friction, turbulence, wave breaking, and other hydrodynamic losses. For conventional vertical breakwaters, K_r usually reaches a high value, approximately 0.90–1.00 under non-breaking wave conditions, increasing standing waves, hydrodynamic pressure, and the risk of local scour at the breakwater toe [5]. For breakwaters integrated with wave energy conversion devices, part of the incident wave energy is absorbed and converted into useful energy. In this case, the energy balance equation is extended as follows [6], [8]:

$$1 = K_r^2 + K_d^2 + K_t^2 + \eta_{abs} \quad (2)$$

where η_{abs} is the fraction of energy absorbed by the WEC/PTO (Wave Energy Converter/ Power Take-Off) system. For vertical-wall or closed caisson breakwater configurations, the transmitted wave component can be considered negligible ($K_t \approx 0$), therefore:

$$1 = K_r^2 + K_d^2 + \eta_{abs} \quad (3)$$

In the integrated WEC system, part of the incident wave energy is absorbed by the PTO mechanism, reducing the overall reflected component. Therefore, the effectiveness of the system is evaluated through the reduction in the reflection coefficient, the increase in absorbed energy, and the reduction in wave loads acting on the structure.

3) Wave–structure interaction simulation model.

Wave–structure interaction was simulated in ANSYS Fluent using an incompressible two-phase water–air flow model. The free surface was tracked using the VOF method, combined with the k-ω SST (Shear Stress Transport) turbulence model to describe the near-wall boundary layer and regions with large velocity gradients, where the pressure distribution and hydrodynamic loads acting on the structure are governed.

The computational domain was a three-dimensional wave flume with a length of 9 m, a height of 2.8 m, and a still water level of 0.35 m. The structure was modeled as a vertical breakwater with a trapezoidal cross-section, a height of 1.4 m, a bottom width of 0.9 m, a top width of 0.5 m, and a width of 3 m. The incident wave was a regular wave with $H = 0.15\,m$, $T = 1.3\,s$, and $\lambda = 2\,m$. The inlet boundary was used for wave generation, the outlet boundary was set as a pressure outlet combined with a wave damping zone, while the bottom and structural surfaces were assigned no-slip wall conditions. The computational domain was discretized using a structured mesh of approximately 1.2×10^5 cells. The problem was solved in unsteady mode with $\Delta t = 0.005\,s$ over a total duration of 15 s, with residual convergence of 10^{-3}–10^{-4}. The extracted quantities included pressure distribution, mean pressure, local maximum pressure, and hydrodynamic force on the front face of the structure [7].

4) Simulation results and data processing.

The CFD (Computational Fluid Dynamics) results show that the pressure on the front face of the structure varies periodically after the transient stage, consistent with the characteristics of the incident regular wave. After scaling according to Froude similarity with a geometric scale ratio of $\lambda_L = 10$, the prototype mean pressure reaches approximately 5.5 kPa, the local maximum pressure reaches 38.1 kPa, and the resultant hydrodynamic force fluctuates within the range of 2.3–3.0 MN. Compared with linear Airy wave theory, the difference in mean pressure is approximately 25%, while the pressure amplitude difference is less than 10%, indicating that the model has acceptable reliability for load analysis and energy absorption assessment [4], [7].

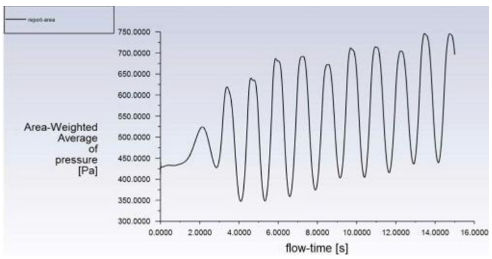

Figure 1. *Graph of results: Average pressure as a function of area versus flow time.*

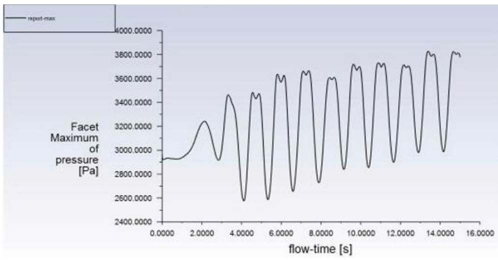

Figure 2. *Graph of results: Maximum pressure as a function of flow time.*

To evaluate the energy absorption capability, the ratio of the force acting on the panel to the force acting on the entire wall face was used as an equivalent absorption coefficient:

$$K_a \approx C = \frac{F_p}{F_w} \tag{4}$$

Assuming that the transmitted wave component through the breakwater is negligible, the equivalent reflection coefficient is determined by:

$$K_r = \sqrt{1 - K_a} \tag{5}$$

The results show that for small waves $H = 1\,m$, the panel almost covers the entire load-bearing region, resulting in $K_a \approx 1.000$and $K_r \approx 0$. As the wave height increases to $H = 4.0\,m$, the absorption coefficient decreases to $K_a = 0.749$ corresponding to $K_r = 0.501$. For large waves $H = 6\,m$, K_a decreases to 0.632 and K_r increases to 0.607. This trend indicates that the absorption efficiency decreases when part of the load-bearing water column extends beyond the effective working range of the panel.

Compared with conventional vertical breakwaters, which tend to produce strong reflection, the integrated breakwater shows the ability to reduce reflected wave energy by converting part of the wave energy into mechanical oscillation and hydraulic energy in the PTO system. The overall results show that the energy-absorbing breakwater can reduce the reflection coefficient by approximately 20–30% and reduce wave loads by approximately 15–25% compared with conventional structures. However, the coefficients K_a and K_r are only derived at the pre-feasibility level from the ratio of the force acting on the panel and therefore need to be further verified using a coupled CFD–PTO model and physical model experiments.

B. Hydraulic Power Take-Off Design and Mechanical Energy Conversion.

1) Hydrodynamic basis for the energy-absorbing panel on the breakwater.

This next part of the study considers the calculation of wave loads and the potential energy acting on an energy-absorbing panel installed on the seaward face of a vertical breakwater. This model is developed for a computational wall strip with a width of $B = 3\,m$, a panel height of $6\,m$, under the design water level of $+1.75\,m$and a seabed elevation in front of the wall of $-3\,m$. Therefore, the design water depth at the structure toe is $d = 1.75 - (-3.0) = 4.75\,m$. The panel is arranged from elevation $-3.0\,m$ to $+3.0\,m$, corresponding to $z_b = -4.75\,m$and $z_t = +1.25\,m$in the coordinate system with the origin at the design water level. The investigated wave-height range is $H = 0.5–9.0\,m$, under the condition of waves incident normally to the wall.

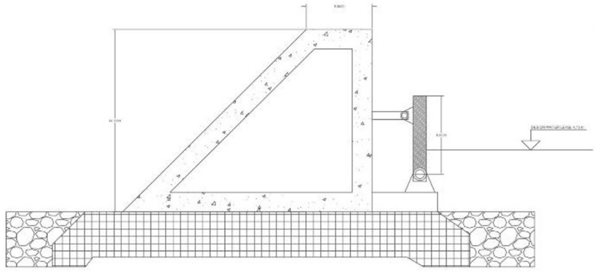

Figure 3. *Computational cross-section schematic.*

In terms of methodology, the wave load is calculated using two branches depending on the wave state at the structure toe. For non-breaking wave conditions, the model uses linear wave theory combined with full reflection at the vertical wall. For wave heights larger than the preliminary breaking threshold, the load is determined using the Goda–Takahashi pressure distribution for vertical walls. The branch-transition threshold is determined using the depth-dependent breaking index: $H_b = 0.78d = 3.705$. Therefore, the cases $H \leq 3.5\,m$are considered as the non-breaking branch, while the cases $H \geq 4.0\,m$ are shifted to the breaking-wave branch. The wave parameters are determined from the assumed deep-water wave steepness: $s_0 = \frac{H}{L_0} = 0.03$.

After determining the representative wave period, the wavelength at the structure is solved through the dispersion equation:

$$\omega^2 = g.k.\tanh(kd)\,;\; L = \frac{2\pi}{k} \tag{6}$$

The incident wave energy and incident wave power over the width B are calculated by:

$$E = \frac{1}{8}\rho g H^2;\; P_{inc} = E c_g B \tag{7}$$

In the non-breaking branch, the dynamic pressure at the vertical wall is determined according to the reflected Airy distribution:

$$p_{NB}(z) = \rho g H \frac{\cosh\,[k(z+d)]}{\cosh\,(kd)} \tag{8}$$

The horizontal force acting on the panel is calculated by integrating the pressure distribution over the panel height. To evaluate the extent to which the panel utilizes the wave load compared with the entire wall strip, the study uses the load coverage index:

$$Capture = \frac{F_{panel}}{F_{wall}} \tag{9}$$

The calculation results show that the lowest panel placement option, namely from elevation $-3.0\,m$to $+3.0\,m$, provides the highest load coverage efficiency within the investigated wave range. For small waves, the panel almost covers the entire load acting on the wall strip. As the wave height increases, the pressure region above the panel increases, causing the proportion of the load covered by the panel to gradually decrease.

Wave height	Property	Fpanel	Capture	Technical signifance
0.5 m	Non-breaking	40.20 kN	100.00%	The panel covers the entire wave load
4.0 m	Breaking wave	665.52 kN	74.90%	The beginning of the transition to the Goda branch
6.0 m	Breaking wave	1,257.46 kN	63.23%	The panel still carries the main load
9.0 m	Breaking wave	2,752.90 kN	51.17%	The largest load case in the survey

Table 1: *Wave force on the panel and load coverage ratio with respect to wave height.*

These results show that the 6 m-high panel is capable of capturing most of the wave load in the small-to-moderate wave range, especially for $H \leq 4\,m$. However, for larger wave conditions, particularly from $H = 6\,m$upward, the proportion of the load outside the panel region increases significantly. This indicates that arranging the panel from the seabed in front of the wall upward is reasonable at the pre-feasibility stage, but further verification using a dynamic model or wave flume experiments is required if the design is developed in detail.

2) Mechanical–Hydraulic Design and Sizing of the PTO System.

With the vertical breakwater configuration, waves act directly on the $3 \times 6\,m$ energy-absorbing panel. At the design wave condition $H = 7\,m$, the total force on the panel reaches $1659.15\,kN$. This force generates a moment around the bottom hinge and is transmitted to the cylinder through a lever arm of $a = 4.5\,m$, with the axial force determined by:

$$F_c = \frac{F_{panel} \cdot y_R}{a} \quad (10)$$

The results show that the cylinder force reaches approximately $1094.78\,kN$. With a pressure limit of $p_{max} = 35\,MPa$, the required piston area is calculated as:

$$A_c = \frac{F_c}{p_{max}} \quad (11)$$

Accordingly, the hydraulic cylinder is selected with a bore diameter of 200 mm and a rod diameter of 120 mm. The cylinder body uses 42CrMo4 + QT steel to ensure pressure resistance and fatigue strength, while the piston rod uses Duplex 2205 stainless steel to improve corrosion resistance in the marine environment.

The accumulator is used to store intermittent energy from waves and release it as a more stable flow to the turbine. The gas compression relationship in the accumulator is described by $pV^n = const$, with the stored energy given by:

$$W = \frac{p_2.V_2 - p_1.V_1}{n-1} \quad (12)$$

The accumulator has a nominal gas volume of 15 L, a nitrogen recharge pressure of 1.35 MPa, and is protected by a 38 MPa relief valve. At the wave condition $H = 7\,m$, the amount of oil charged into the accumulator reaches approximately 12.72 L. Since the piston receives compressive force from only one side, a charge pump is used to supply return oil to the cylinder chamber with a peak flow rate of approximately 525 L/min.

Figure 4*. 3D model of the hydraulic piston system and hydraulic accumulator*

The high-pressure oil flow is then directed through a nozzle to transmit energy to the Pelton turbine. The oil jet velocity and wheel peripheral velocity are determined by:

$$V_j = C_v\sqrt{\frac{2p}{\rho}};\ U = K_u.V_j \quad (13)$$

With $C_v = 0.98$, $K_u = 0.46$, $\rho = 870\,kg/m^3$, and a maximum pressure of $p = 34.84\,MPa$, the Pelton runner diameter is calculated as:

$$D_t = \frac{U.60}{\pi RPM} \approx 487.4\,mm \quad (14)$$

Therefore, a Pelton turbine with a nominal diameter of 490 mm is selected to achieve the target rotational speed of approximately 5000 RPM and ensure stable operation under varying wave loads.

Wave height	Force on panel	System pressue	Restoring velocity	Turbine speed (RPM)
0.5 m	40.20 kN	~0.57 MPa	0 m/s	0
1.0 m	118.76 kN	1.68 MPa	60.9 m/s	~1,098
2.0 m	297.08 kN	5.56 MPa	110.8 m/s	~1,997
4.0 m	665.52 kN	13.84 MPa	174.8 m/s	~3,151
6.0 m	1,257.46 kN	26.36 MPa	241.2 m/s	~4,348
7.0 m	1,699.15 kN	34.84 MPa	277.4 m/s	~5,000

Table 2: *Operating parameters of the Pelton turbine with a diameter of 490 mm.*

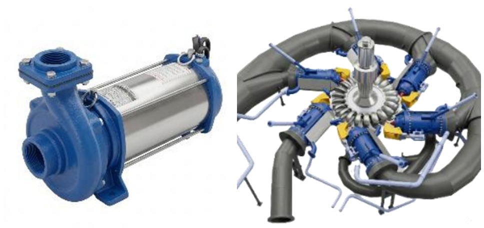

Figure 5*. 3D model of the hydraulic charge pump and Pelton turbine.*

3) Verification simulation using ANSYS CFD.

To confirm the absolute reliability of the mathematical model, all boundary parameters, including pressure $p$and jet velocity V_j, were extracted and set up in the computational fluid dynamics simulation environment (ANSYS CFD).

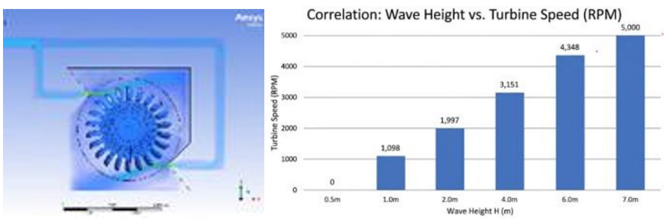

Figure 6*. ANSYS CFD simulation results for turbine rotational speed calculation.*

The simulation results of the velocity field and fluid interaction on the Pelton runner with a diameter of 490 mm show good agreement with the analytical calculation. Under the critical condition of $H = 7\ m$ and a pressure of 34.84 MPa, the turbine rotational speed in the simulation converges stably at approximately 5000 rpm, closely matching the theoretical prediction. This cross-verification result shows that the parameter selection method is reliable, while also confirming the feasibility of the system in converting wave energy into continuous rotational mechanical energy for high-power electricity generation.

4) Conclusion.

The calculation and simulation results show that the hydraulic PTO system can maintain a turbine speed range of approximately 1,000–5,000 rpm within the investigated wave range of 1–7 m. This provides the basis for integrating the generator in the next step; however, further verification using a coupled dynamic model and experimental testing is still required.

C. Wave-to-Wire Power Conversion and Energy Management.

1) Wave-to-wire energy conversion structure.

The stability of availability requires the development of a synchronized wave-to-wire model to convert the variable energy flow into standard electrical power [6], [8]. This is an important foundation in the development of wave energy conversion devices, allowing the overall efficiency to be evaluated from an interdisciplinary perspective involving hydrodynamics, mechanics, and electrical engineering.

In terms of operating principle, wave energy is converted into oscillatory mechanical energy or pneumatic/hydraulic energy through the primary absorber, then transmitted through the PTO system to generate suitable motion for the electrical generator, commonly a PMSG, DFIG (Doubly Fed Induction Generator), or linear generator. Since the generator output has variable amplitude and frequency depending on wave conditions, the electrical power is processed through an AC–DC–AC structure consisting of a rectifier, DC-link, and inverter to stabilize voltage, frequency, and power quality before being stepped up through a transformer and transmitted to the national power grid.

2) Wave energy calculation.

Ocean waves are formed through the transfer of energy from wind to the ocean surface. When wind blows with high intensity over a sufficiently long distance, the energy accumulated in the waves increases significantly, creating favorable conditions for energy harvesting. Therefore, quantifying wave power is a fundamental step in designing a wave-to-electricity energy conversion system. For regular waves, the wave power per unit crest width is determined by [4], [6]:

$$P = \frac{1}{8}\rho_{water} g C_g H^2 \tag{15}$$

where ρ_{water} is the density of water, g is gravitational acceleration, H is the wave height, and C_g is the group velocity, which characterizes the propagation speed of wave energy. The group velocity is determined by:

$$C_g = \frac{1}{2}\left[1 + \frac{2kh}{\sin h(2kh)}\right]\frac{\lambda}{T} \tag{16}$$

where k is the wave number, h is the water depth, λ is the wavelength, and T is the wave period. This expression shows that the energy propagation velocity strongly depends on water depth conditions, thereby directly affecting the exploitable power. In shallow water conditions $(h < 0.5\lambda)$, the wavelength can be approximated by [4], [6]:

$$\lambda = \frac{gT^2}{2\pi}\left(\tan h\left[\left(\frac{4\pi^2 h}{gT^2}\right)^{3/4}\right]\right)^{2/3} \tag{17}$$

Conversely, in deep water $(h > 0.5\lambda)$, the expressions are significantly simplified:

$$\lambda = \frac{gT^2}{2\pi} \tag{18}$$

$$C = \frac{\lambda}{T} = 2C_g \tag{19}$$

Then, in order to reduce computational complexity while still ensuring acceptable accuracy, the wave power can be rewritten as [4], [6]:

$$P = \frac{1}{32\pi}\rho_{water} g^2 H^2 T \tag{20}$$

where H_s is the significant wave height, T_e is the energy period, and $C_g(T_e, h)$ is the group velocity. In some studies, the energy period can be assumed to be approximately equal to the peak period to simplify the calculation [9]:

$$P \approx \frac{\rho_{water} g^2}{64\pi} H_s^2 T_p \tag{21}$$

When the pressure in the accumulator reaches the design threshold, the energy is released through a high-pressure fluid flow passing through the hydraulic turbine. The hydraulic power supplied to the turbine is determined by:

$$P_{hyd} = p_h \cdot Q \tag{22}$$

where Q is the flow rate. The electrical output power is determined by:

$$P_{elec} = \eta_{turb} \cdot \eta_{gen} \cdot P_{hyd} \tag{23}$$

where η_{turb} and η_{gen} are the efficiencies of the turbine and the generator, respectively.

3) Practical results.

Based on the hydraulic and mechanical calculations, the output power of each module ranges from approximately 13.93–288.95 kW; therefore, a PMSG generator with a rated power of about 300 kW is selected to ensure reserve capacity and stable operation. The back-to-back system is designed with a reserve capacity of 10–20% compared with the generator, allowing maximum wave energy harvesting, achieving an overall efficiency of approximately 80–85%, and meeting the requirements for stable grid connection. The selection results and the simulation of the electrical energy conversion process using MATLAB/Simulink show that each module can generate from several tens to nearly 300 kW, corresponding to hundreds of kWh to several MWh under wave conditions from 1–7 m. With the wave potential of the central coast and the demand for coastal protection in Quang Tri, this area is suitable for developing an integrated breakwater wave power system.

The study shows that wave energy harvesting is not only a coastal protection solution but also opens a strategic approach for future coastal infrastructure. With a potential power of up to 288.95 kW for each module, the system can supplement a significant power source for the national grid, serving coastal infrastructure and smart cities. In the context that fossil energy sources such as coal, oil, and gas are increasingly revealing their limitations, wave energy is a clean and highly potential renewable energy source that can be directly integrated into infrastructure works to create dual value in terms of engineering, economy, and environment.

D. Coastal Infrastructure Integration and Deployment Strategy.

1) Shifting the coastal design paradigm.

Figure 7. *Overall perspective of the multifunctional breakwater.*

In the context of smart cities, coastal protection infrastructure requires the intersection between hydraulic engineering and multidimensional planning thinking. The breakwater system integrated with the energy converter (WEC-PTO) marks a design turning point: transforming passive concrete blocks into an organic structure that both eliminates destructive wave energy, generates renewable energy, and creates iconic public space.

2) Architectural morphology and hydrodynamic basis.

Figure 8*. Organic integrated breakwater structure.*

The flexibility of the hydraulic transmission modules allows the breakwater alignment to adapt to all types of terrain forms (concave alignment, convex alignment) without disrupting the landscape. The curved profile and stepped cross-sections of the breakwater surface are not random design lines, but the result of an optimization process through multi-flow simulation models as CFD, MIKE 21, HEC-RAS (Hydrologic Engineering Center's River Analysis System).

The breakwater alignment profile and PTO module arrangement need to be optimized through hydrodynamic simulations to reduce reflection, limit wave overtopping, and create a relatively stable water area behind the structure. Public spaces should only be arranged in areas that meet safety requirements regarding wave loads, settlement, and operation and maintenance.

3) Benchmarking against international design standards.

The design needs to be compared with maritime standards such as BS 6349 (British Standard 6349) and the Coastal Engineering Manual to check structural stability, wave loads, wave overtopping, settlement, and operational safety. Public facilities must be arranged outside areas subjected to dangerous dynamic loads and must ensure that they do not obstruct maintenance of the PTO system.

Figure 9. *Layout of the hydraulic PTO system.*

4) "Placemaking" and urban economic dynamics.

When appropriately planned, the WEC-integrated breakwater alignment can serve as a coastal linear park, combining shoreline protection, on-site power generation, and public space creation. However, socio-economic effectiveness needs to be evaluated separately in future studies.

III. Integrated Discussion, Limitations and Future Work.

When appropriately planned, the WEC-integrated breakwater alignment can serve as a coastal linear park, combining shoreline protection, on-site power generation, and public space creation. However, socio-economic effectiveness needs to be evaluated separately in future studies.

CONCLUSION

This study proposes a breakwater system integrated with wave energy harvesting to combine shoreline protection and on-site renewable power generation. The preliminary simulation and calculation results show that the system can reduce the reflection coefficient by approximately 20–30%, reduce wave loads by approximately 15–25%, and achieve a potential power of up to 288.95 kW for each module. The system has the capability to supply power to coastal infrastructure, sensors, lighting, and smart city applications. However, the results are currently at the pre-feasibility level and need to be further verified through model experiments, coupled CFD–PTO–generator simulations, and field testing. This approach opens a direction for the development of multifunctional coastal infrastructure, contributing to energy transition and the net-zero emission target.

Acknowledgment

The authors would like to sincerely thank Assoc. Prof. Dr. Vo Ngoc Duong for his guidance, professional comments, and technical support throughout the implementation of this study. The authors would also like to thank the relevant faculties of the University of Danang for their support during the development of the multidisciplinary design framework for the breakwater system integrated with wave energy harvesting.

References

[1] Intergovernmental Panel on Climate Change, Climate Change 2021: The Physical Science Basis. Cambridge, U.K.: Cambridge University Press, 2021.

[2] National Centers for Environmental Prediction, "Climate Forecast System Reanalysis (CFSR)," National Oceanic and Atmospheric Administration, 1979–present.

[3] Quang Tri People's Committee, Report on Marine and Island Resources and Environment of Quang Tri Province. Quang Tri, Vietnam, 2020.

[4] U.S. Army Corps of Engineers, Coastal Engineering Manual. Washington, DC, USA: U.S. Army Corps of Engineers, 2002.

[5] B. Zanuttigh and J. W. van der Meer, "Wave reflection from coastal structures in design conditions," Coastal Engineering, vol. 55, no. 10, pp. 771–779, 2008.

[6] J. Falnes, Ocean Waves and Oscillating Systems: Linear Interactions Including Wave-Energy Extraction. Cambridge, U.K.: Cambridge University Press, 2002.

[7] ANSYS, Inc., ANSYS Fluent Theory Guide. Canonsburg, PA, USA: ANSYS, Inc., 2023.

[8] M. A. Jusoh, M. Z. Ibrahim, M. Z. Daud, A. Albani, and M. Z. Yusop, "Hydraulic power take-off concepts for wave energy conversion system: A review," Energies, vol. 12, no. 23, Art. no. 4510, 2019.

[9] B. Multon, Ed., Marine Renewable Energy Handbook. Hoboken, NJ, USA: Wiley, 2012.